Research Article J. Electrochem. Sci. Technol., 2019, 10(4), 416-423

# An Oxalic Acid Sensor Based on Platinum/Carbon Black-Nickel-Reduced Graphene Oxide Nanocomposites Modified Screen-Printed Carbon Electrode

Kamolwich Income[1,2], Nalin Ratnarathorn[1,2], Suwaphid Themsirimongkon[3], and Wijitar Dungchai[1,2]*

[1] *Organic Synthesis, Electrochemistry & Natural Product Research Unit, Department of Chemistry, Faculty of Science, King Mongkut's University of Technology Thonburi, Prachautid Road, Thungkru, Bangkok 10140, Thailand*

[2] *Applied Science & Engineering for Social Solution Unit, Faculty of Science, King Mongkut's University of Technology Thonburi, Prachautid Road, Thungkru, Bangkok 10140, Thailand*

[3] *Department of Chemistry, Faculty of Science, Chiang Mai University, Chiang Mai 50200, Thailand*

**ABSTRACT**

A novel non-enzymatic oxalic acid (OA) sensor based on the platinum/carbon black-nickel-reduced graphene oxide (Pt/CB-Ni-rGO) nanocomposite is reported. The nanocomposites were prepared by the ethylene glycol reduction method. Their morphology and chemical composition were characterized by scanning electron microscopy (SEM), energy dispersive X-ray spectroscopy (EDX) and transmission electron microscopy (TEM). The results clearly demonstrated the formation of the Pt/CB-Ni-rGO nanocomposite. The electrocatalytic activity of the Pt/CB-Ni-rGO electrode was investigated by cyclic voltammetry. It was determined that the appropriate amount of Pt enhanced the catalytic activity of Pt for oxalic acid electro-oxidation. Moreover, the modified electrode was determined to be highly selective for oxalic acid without interference from compounds commonly found in urine including uric acid and ascorbic acid. The chronoamperometric signal gave a wide linearity range of 20 μM-60 mM and the detection limit (3σ) was found to be 2.35 μM. The proposed method showed high selectivity, stability, and good reproducibility and could be used with micro-volumes of sample for the detection of oxalic acid. Finally, the oxalic acid content in artificial and control urine samples were successfully determined by our proposed electrode.

**Keywords :** Oxalic Acid, Platinum Nanoparticle, Carbon Black, Reduced Graphene Oxide

*Received : 4 May 2019, Accepted : 28 July 2019*

## 1. Introduction

The amount of oxalic acid in urine and plasma is important for the diagnosis and monitoring of primary hyperoxaluria, malabsorption, urolithiasis, ileal disease, and steatorrhoea [1]. The oxalic acid is 0.80-2.50 μM in normal human plasma [2] and 20-30 mg/24 h (159-238 μM) in normal human urine [3]. As a result of endogenous synthesis under pathological conditions or the increased intake of dietary oxalate, oxalate accumulates in the body causing hyperoxaluria with generation of calcium oxalate urinary stones. This results in increased excretion of urinary oxalate in the form of stone [4]. The accurate determination of oxalic acid has attracted considerable interest for the diagnosis and prevention of kidney stone formation [5]. Consequently, a more efficient and simple method for measuring urinary oxalic acid is desired. Several methods exist for oxalate determination such as co-electroosmotic capillary electrophoresis [6], high-performance liquid chromatography [7], flow injection spectrophotometry [8], chemiluminescence [9], ion chromatography [10] and enzyme-based biosensors [11]. These methods provide high sensitivity and selectivity. Nevertheless, several of these methods suffer from time-consuming analysis, use of costly instrument and/or insufficient enzyme stability. The measurement of oxalic acid using electrochemical sensing has received more attention

*E-mail address: wijitar.dun@kmutt.ac.th

DOI: https://doi.org/10.33961/jecst.2019.00206

because of its low cost, good detection limit, speed of analysis, ease of miniaturization and simple operation [12,13]. Interfering species that generally impact oxalic acid oxidation include uric acid (UA) and ascorbic acid (AA). To prevent interference, some sensors use chemically and/or physically-modified electrodes such as boron-doped diamond electrode [14] and carbon nanotubes-modified electrode [15]. However, the oxidation of oxalic acid at these electrodes requires a high overpotential [14,15]. Noble metal nanoparticles have generated as electrode modifiers due to their high surface area, electrocatalytic property and stability [16-18].

Platinum (Pt) is well known for its catalytic property towards the oxidation of oxalic acid [19-21]. To obtain higher surface area and decrease the catalyst cost, Pt nanoparticles have been immobilized on the surface of conductive support materials (graphene) [22-25]. Graphene oxide (GO) has been commonly used as a support material because of its high surface area and electrical conductivity. However, during the electrode fabrication GO layers modified with Pt nanoparticles can horizontally stack in itself layer [26]. When the stacking occur, the Pt catalytic sites loss and the diffusion resistance of the reactant molecules increase [26-29]. Here, a carbon black-nickel-reduced graphene oxide (CB-Ni-rGO) support material with Pt nanoparticles has been developed to address these problems. The new material reduces the diffusion resistance while retaining the high electrical conductivity and surface area. CB was used as a spacer between Pt and GO sheets in the catalyst layer [30], while Ni catalyst ions react with hydroxyl surface functional groups of CB and GO via an ionic adsorption process leading to stable nanocomposites.

In this work, the electrochemical behaviors of Pt nanoparticles decorated on carbon black-nickel-reduced graphene oxide modified screen-printed carbon electrode (Pt/CB-Ni-rGO/SPCE) are described. The electrocatalytic activity of modified electrodes have been investigated towards oxidation of oxalic acid. Pt/CB-Ni-rGO/SPCE were successfully used for the detection of oxalic acid in biological samples.

## 2. Experimental

### 2.1 Materials and chemicals

Ethylene glycol, sodium chloride and potassium chloride were purchased from Ajax Finechem Pty Ltd. Oxalic acid, ascorbic acid, calcium chloride, citric acid, sodium hydrogen carbonate, sodium sulphate, sodium hydrogen phosphate and sodium dihydrogen phosphate were received from BDH Prolabo. Graphite (99.8%), carbon black (Vulcan XC 72R) and nafion were purchased from the Fuel Cell Earth (USA). The solutions were prepared with deionized water (a Millipore Milli-Q water system). The standard solutions of platinum and nickel at a concentration of 1,000 mg $L^{-1}$ (AAS standard) were purchased from Merck.

### 2.2 Instrumentation

Cyclic voltammetry (CV) and chronoamperometry (CA) measurements were carried out on a EmStat3 potentiostat (PalmSens, Netherlands) controlled by the PSTrace 5.3 software coupled with screen-printed carbon electrodes (SPCEs) (Quasense, Thailand). The SPCEs consisted of a silver/silver chloride as the reference electrode, carbon for the auxiliary electrode and a 3 mm diamter carbon working electrode with a polycarbonate support. Scanning electron microscopy (SEM) was obtained using JEOL JSM-6610LV scanning electron microscope that was attached with OXFORD INCA350 to perform an energy dispersive X-ray (EDX) spectrum. A transmission electron microscopy (TEM) images of the material was obtained with JEOL-2010 instrument (JEOL Ltd., Japan).

### 2.3 Preparation of Pt/CB-Ni-rGO

Natural graphite powder GO was used to synthesize GO using our method [31]. Then, preparation of CB-Ni-rGO was started by dispersing 33, 50 and 67 mg of GO slurry in 70 mL of deionized water for 30 min in an ultrasonicator. Next, quantities of 5, 10, 15 and 20 mL of Ni standard solution were added into GO suspension followed by sonication for 30 min. After that, 33, 50 and 67 mg of carbon black (CB) were added into the mixture and ultrasonicated for 30 min to form a homogeneous CB-Ni-rGO suspension. Pt/CB-Ni-rGO was prepared in the next step. Accurate quantities (5, 10, 15 and 20 mL) of Pt standard solution were added into a homogeneous CB-Ni-rGO suspension and followed by sonicated for 30 min. After that, 70 %v/v ethylene glycol was added into the mixture and stirred vigorously for 5 min. Then, the solution was adjusted until pH 11 with 1 M sodium hydroxide, heated up to 120 °C with stirring for 3 h,

and left at room temperature. After washing the mixture until the solution pH was neutral, the Pt/CB-Ni-rGO suspended precipitate was collected by centrifugation and dried in an oven at 60°C.

SPCEs were modified with Pt/CB-Ni-rGO nanocomposite by the drop casting method. Five microliters of the Pt/CB-Ni-rGO nanocomposite solution that was 2 mg of Pt/CB-Ni-rGO nanocomposite in 1 mL of 6% nafion solution was dropped onto the working electrode and allowed to dry completely at room temperature for overnight.

### 2.4 Electrochemical measurement of oxalic acid

The cyclic voltammetry (CV) was applied to study the electrochemical performance of the electrode by cycling the potential between 0.0 and +1.5 V at 50 mV $s^{-1}$. The linear range of experiment was studied by chronoamperometry (CA) at the potential level of +0.70 V versus Ag/AgCl by recorded steady state anodic currents at 100 s.

### 2.5 Urine sample analysis

To demonstrate the utilization of modified electrode, an artificial urine sample was prepared following S. Chutipongtanate et al. [32]. The known amount of oxalic acid was spiked in the artificial urine sample 1 for the healthy (100 μM oxalic acid) and high level of oxalic acid for unhealthy populations in the artificial sample 2-5 (5,000, 15,000, 25,000 and 60,000 μM oxalic acid, respectively). The control samples level I and level II (liquid assayed urinalysis Lot. UB1519021A for level I and Lot. UB1519022A for level II) were purchased from ThermoScientific (Waltham, MA). Liquid assayed urinalysis control samples level I and II spiked with oxalic acid at 200 and 400 μM were represented to the healthy and unhealthy populations, respectively. Prior to measurement, artificial urine and liquid assayed urinalysis control samples were pretreated with 0.05 M $H_2SO_4$ to adjust the supporting solution as same with calibration condition.

## 3. Results and Discussion

### 3.1 Surface characterization of Pt/CB-Ni-rGO/SPCE

The morphology of the bare SPCE surface shows particles dispersed across the electrode surface (Fig. S1a). SEM images of the synthesized GO (Fig. S1b), Ni-rGO (Fig. S1c), CB-Ni-rGO (Fig. S1d) and Pt/CB-Ni-rGO (Fig. S1e) were also obtained. As can be seen in Fig. S1c, the structure of the GO surface with Ni deposited is different from GO surfaces without Ni deposited. The structure of electrodes with CB-Ni-rGO has two-phases, with some flat and some rougher (Fig. S1d). Then, the element on Pt/CB-Ni-rGO nanocomposite was confirmed by SEM-EDX (Fig. S1e, f). The spectrum showed the presence of carbon (C), oxygen (O), nickel (Ni) and platinum (Pt), indicating the formation of a high purity composite. Fig. 1a, b, c illustrated TEM image of the nano-sized particles (2.89±0.54 nm) of an alloy (Ni and Pt) that were loaded into the carbon composites. Moreover, Table S1 shows the highest active surface area of Pt/CB-Ni-rGO modified electrodes which were calculated from the peak currents of $[Fe(CN)_6]^{4-/3-}$ in Fig. S2 using Randles-Sevick equation [33].

### 3.2 Electrochemical study of oxalic acid at the Pt/CB-Ni-rGO/SPCE

The electrochemical oxidation of oxalic acid were studied on modified electrodes. The cyclic voltammograms of 10 mM oxalic acid on modified electrodes are presented in Fig. 2. The anodic peak of oxalic acid on GO-modified SPCE did not appear comparing the anodic peak current from the bare SPCE ($i_p$ = 83.67±3.51 μA), likely due to aggregation of GO film on SPCE and decrease of the conductivity (Fig. 2a, b). Ni catalyst ions reacting with hydroxyl surface functional groups of GO lead to an increase in the anodic current relative to the GO-modified SPCE (Fig. 2c). The CB-Ni-rGO modified SPCE generated a lower potential of oxalic acid oxidation (around +1.10 V, 96.33±2.08 μA) compared to the GO-modified SPCE (around +1.20 V) (Fig. 2d). The results indicate that the CB and Ni-decorated on GO causes catalytic oxidation of oxalic acid. Pt/CB-Ni-rGO modified SPCE showed a highest anodic current 132.33±2.52 μA) than those electrodes at the lowest potential (around +0.60 V) because the CB-Ni-rGO gave a stable structure of Pt nanocomposites and prevented stacking of graphene layers (Fig. 2e). The low oxidation potential of oxalic acid oxidation could provide the interference free for chronoamperometric detection in the future. Fig. 3 shows the schematic mechanism of electrocatalytic oxidation of oxalic acid in $H_2SO_4$ solution at the Pt/CB-Ni-rGO. Finally, the applied potential for chronoamperometric measurements was studied. Table S2 shows highest cali-

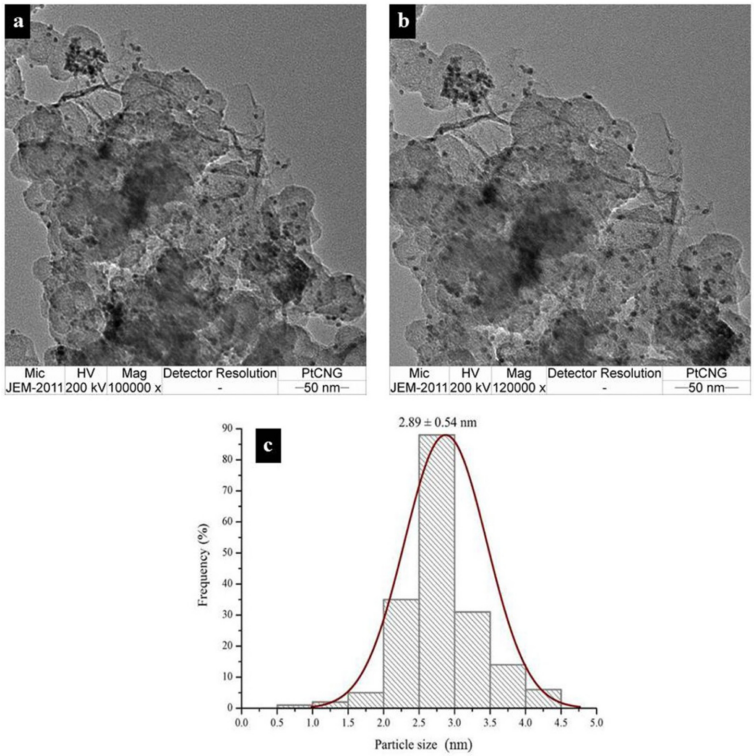


**Fig. 1.** TEM image of Pt/CB-Ni-rGO at (a) 100000X, (b) 120000X and (c) histogram for alloy an (Ni and Pt) nanoparticle sizes.

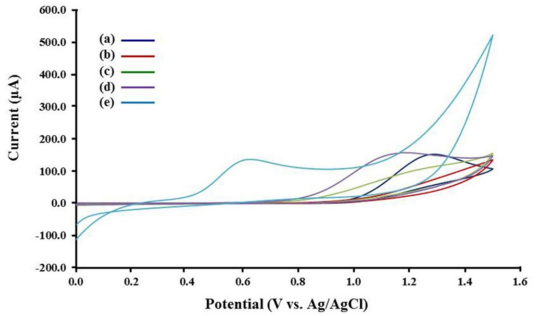


**Fig. 2.** Cyclic voltammograms of (a) bare SPCE, (b) GO/SPCE, (c) Ni-rGO/SPCE, (d) CB-Ni-rGO/SPCE and (e) Pt/CB-Ni-rGO/SPCE in 0.05 M $H_2SO_4$ containing 10 mM oxalic acid.

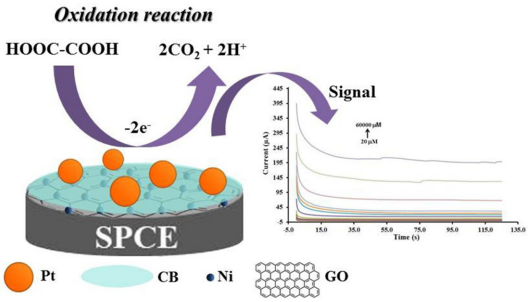


**Fig. 3.** Illustration of nonenzymatic oxalic acid sensing mechanism using Pt/CB-Ni-rGO composites.

bration slopes at +0.70 V applied potentials. Thus, +0.70 V was chosen as the applied potential in the analytical performance study and application.

Next, the diffusion controlled mass transfer process of Pt/CB-Ni-rGO modified on SPCE was investigated using CV in 10 mM $[Fe(CN)_6]^{4-/3-}$ at various scan rates (10-160 mV $s^{-1}$) (Fig. 4a). As shown in Fig. 4b, both cathodic and anodic peak current responses are directly propotional to square root of scan rate ($v^{1/2}$), following the Randles-Sevick equation (1) [33-35]. It indicated that a diffusion controlled mass transfer process occurs on Pt/CB-Ni-rGO modified SPCE [36].

$$i_p = (2.99 \times 10^5)\, n^{3/2} A D^{1/2} v^{1/2} C \quad (1)$$

where n is the electrons exchanged number of the

redox reaction and A is the active area of the working electrode ($cm^2$). The diffusion coefficient (D ($cm^2$ $s^{-1}$)) of $[Fe(CN)_6]^{4-/3-}$ equals to $6.70\times10^{-7}$ $cm^2$ $s^{-1}$ and the bulk concentration of the electroactive species is C (mol $cm^{-3}$). The voltage scan rate (V $s^{-1}$) is ν.

### 3.3 Optimization of oxalic acid detection

The pH of analyte solution has an effect on the electrochemical oxidation of oxalic acid [15]. The effect of pH on electrooxidation of oxalic acid at the surface of Pt/CB-Ni-rGO was therefore investigated using 0.1 M perchloric acid, 0.1 M sulfuric acid, 0.1 M hydrochloric acid and 0.1 M phosphate buffer pH 4.0-6.0. The voltammetric responses of oxalic acid are shown in Fig. S3. The results show that the electrooxidation of oxalic acid occurred at pH lower than 4.0 when the pH is lower than the $pK_a$ of oxalic acid. The highest electrochemical response was obtained in sulfuric acid. Moreover, the sulfuric acid concentrations were tested in the range of 0.01-0.1 M. It was found that the concentration of sulfuric acid influences the voltammetric response of oxalic acid (Fig. S4). The highest peak current was observed at 0.05 M sulfuric acid solution. At concentrations higher than 0.05 M sulfuric acid, the peak current decreased (Fig. 5a). Therefore, 0.05 M sulfuric acid was selected as the optimum solution for further investigations.

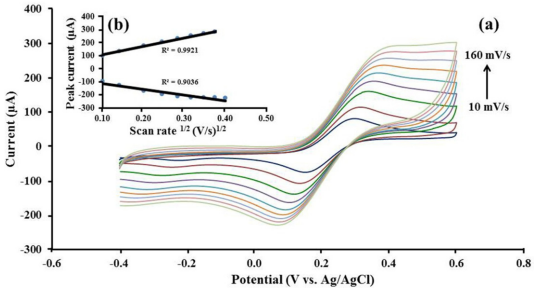


**Fig. 4.** (a) Cyclic voltammograms response of 10 mM $[Fe(CN)_6]^{4-/3-}$ in 1 mM KCl on Pt/CB-Ni-rGO modified SPCE at various scan rates 10, 20, 40, 60, 80, 100, 120, 140 and 160 mV $s^{-1}$. (b) Plot for the peak current versus the square root of the scan rate ($\nu^{1/2}$) in the same solution.

Next, the ratio of CB to rGO was investigated in the range of 1:2, 1:1 and 2:1. Fig. S5 displayed the CVs of 10 mM oxalic acid at the various ratio of CB to rGO. The well-defined oxidation peak of oxalic acid was obtained at 1:1 of CB:rGO (Fig. 5b). Thus, the ratio of CB to rGO of 1:1 was chosen for subsequent studies. The influence of %Ni and %Pt loading on carbon hybrid support were also examined. The oxidation current increased with the increase of %Ni loading until 10% w/w as shown in Fig. S6. According to the excess amount of Ni nanoparticles on carbon hybrid support at the >10% w/w of Ni, the peak current decreased (Fig. 5c). Hence, 10% w/w Ni

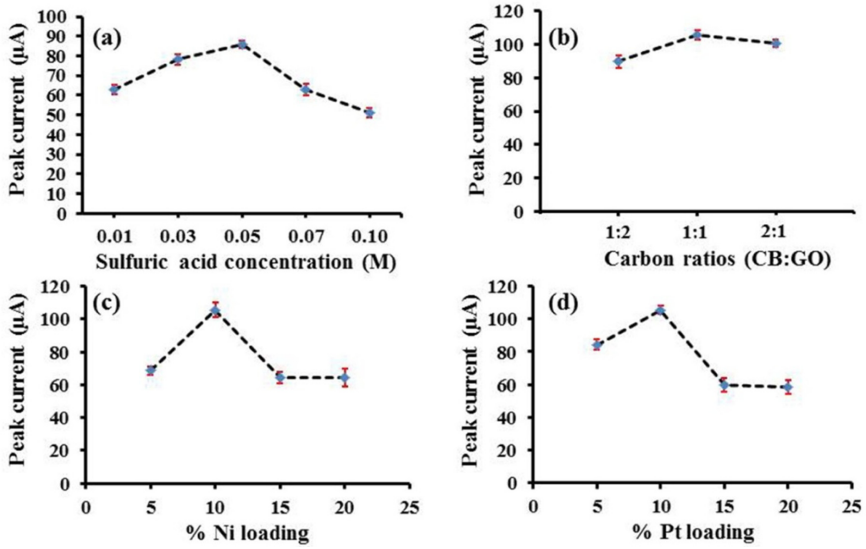


**Fig. 5.** Effect of (a) sulfuric acid concentration for supporting electrolyte, (b) carbon ratio, (c) %Ni loading and (d) %Pt loading on supported material to oxidation peak currents of 10 mM oxalic acid detection.

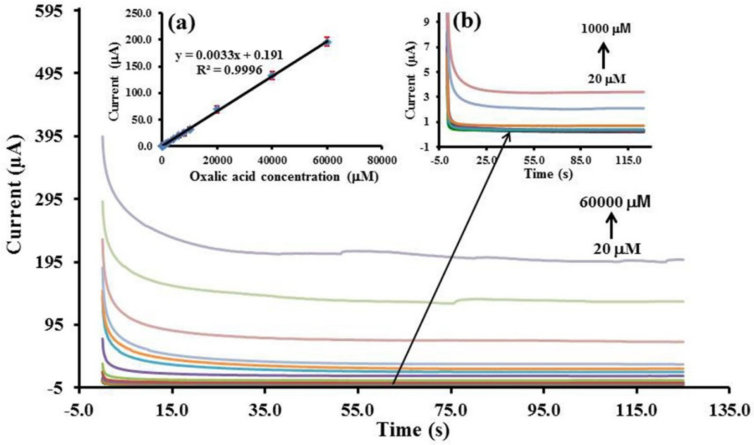


**Fig. 6.** Chronoamperograms at the Pt/CB-Ni-rGO in 0.05 M $H_2SO_4$ containing different concentrations of oxalic acid at +0.70 V versus Ag/AgCl ink. The inset shows (a) the calibration curve for oxalic acid detection and (b) the enlarged chronoamperograms of oxalic acid from 20 to 1,000 µM.

loading was selected for subsequent studies.

The %Pt loading on CB-Ni-rGO also has an effect on the oxalic acid oxidation because the high %Pt cause the aggregation whereas the low %Pt gives the low conductivity. Thus, the %Pt loading were studied in the range of 5-20% w/w. The oxidation current increased with the increasing of %Pt loading until 10% w/w (Fig. S7, 5d) due to the excess amount of Pt nanoparticles on CB-Ni-rGO resulting in the aggregation of Pt nanoparticles. Hence, the loading of Pt on CB-Ni-rGO was selected at 10% w/w.

### 3.4 Analytical performance

Chronoamperometry (CA) was used to study the analytical performance. The steady state anodic current was a linear with the oxalic acid concentration in the range of 20-60,000 µM which the coefficient of linearity ($R^2$) was found to be 0.9996 (Fig. 6). The detection limit was 2.35 µM by calculated concentration from three times to noise (n = 10).

The interferences of common biological species found in urine were studied on the Pt/CB-Ni-rGO modified SPCE. Under the optimal conditions, 200 µM oxalic acid including 1 mM uric acid, 1 mM ascorbic acid, 5 mM citric acid, 1 mM creatinine, 1 µM albumin, 0.005 mM dopamine, 1 mM glucose and 100 mM Urea were studied. The anodic current of oxalic acid in the presence of those species was found in the range of 96-104% when compared to oxalic acid in the absence of those species (Fig. S8). In human urine, oxalic acid typically coexists with common interfering molecules, some of which are electroactive compounds such as ascorbic acid and uric acid. As shown in Fig. S9a, ascorbic acid strongly affected the current response while uric acid had a weaker interference for oxalic acid determination using a bare SPCE. The problem was solved by coating the electrode with Pt/CB-Ni-rGO nanocomposites. Compared to the cyclic voltammograms of both bare SPCE and Pt/CB-Ni-rGO modified SPCE, the currents from ascorbic acid and uric acid (Fig. S9b) oxidation for Pt/CB-Ni-rGO modified SPCE vanished. The Pt/CB-Ni-rGO as a oxalic acid sensor exhibited high selectivity, thus it holds promise for practical applications.

A comparison between the analytical performance of this method and some previous non-enzymatic sensors for the determination of oxalic acid is illustrated in Table S3. Most of previous sensors were applied for food analysis so some of them did not study the interference presenting in biological sample such as urea, citric acid, creatinine, ascorbic acid and uric acid. Only diamond electrode was applied for biological sample (plasma) but the diamond electrode is high cost and needs the complexed insturment for fabricaiton. Our proposed sensors are better in terms of wider linearity with the acceptable detection limits and we also studied the interference of common biological molecules. The SPCE also exhibited over benefits than other bulk electrodes, such as portability, simplicity, disposibility, low-cost, less reagent

**Table 1.** Determination and recoveries of oxalic acid in control urine samples (n=3).

| Samples | Concentration of oxalic acid (μM) | | % Recovery | % RSD |
|---|---|---|---|---|
| | Added | Obtained | | |
| Artificial urine-1 | 100 | 103 | 103 | 0.43 |
| Artificial urine-2 | 5,000 | 4,999 | 100 | 2.50 |
| Artificial urine-3 | 15,000 | 14,434 | 96 | 5.33 |
| Artificial urine-4 | 25,000 | 25,391 | 102 | 3.20 |
| Artificial urine-5 | 60,000 | 63,871 | 106 | 5.81 |
| Control urine level I | 200 | 207 | 104 | 0.86 |
| Control urine level II | 400 | 411 | 103 | 1.52 |

and sample consumption. Therefore our sensor could be useful for urinalysis in the developing country and undeveloping country.

The reproducibility of Pt/CB-Ni-rGO modified electrode was demonstrated using eight separately prepared Pt/CB-Ni-rGO modified SPCEs in 10 mM of oxalic acid. The relative standard deviation (RSD) was found at 1.47% (n=8) so the reproducibility of the proposed electrode was in an acceptable level according to AOAC International standards [37]. Moreover, the stability of the Pt/CB-Ni-rGO modified electrode was investigated during storage over 2 weeks. The anodic current remained stable for 2 weeks due to only about 10% decrease of response current (Fig. S10). Thus, our proposed electrode has high reproducibility and good stability towards the electrooxidation of oxalic acid.

### 3.5 Application

To validate the application of the proposed method, Pt/CB-Ni-rGO was utilized to measurement the artificial urine and control urine samples by chronoamperometry. The analytical results are concluded in Table 1. The recovery precentages of oxalic acid in the artificial urine and control urine samples were found in the range of 96-106. The %RSD of theses experiments was established in the range of 0.43-5.81%. These results show the utility of the Pt/CB-Ni-rGO-modified SPCE for the accurate detection of the oxalic acid in urine samples.

## 4. Conclusions

In this work, the Pt/CB-Ni-rGO nanocomposites modified on SPCEs have been successfully applied for the non-enzymatic determination of oxalic acid. The surface morphology of the Pt/CB-Ni-rGO nanocomposite was characterized by SEM, EDX and TEM. The results clearly demonstrate formation of Pt/CB-Ni-rGO nanocomposites. The nanocomposites were investigated for the electrochemical detection of oxalic acid in 0.05 M $H_2SO_4$. The linear scan rate dependence showed that the system undergoes a diffusion controlled electrode process. When the modified electrode was used to detect oxalic acid by chronoamperometry, a wide linear response in the range of 20 to 60,000 μM with a low detection limit of 2.35 μM was found. The modified electrode was demonstrated to have an increased current response, low interference from common biological molecules, good reproducibility and good stability relative to unmodified SPCEs. Furthermore, the modified electrode was applied to detect oxalic acid in urine samples with accurate results. Therefore, our proposed method could be beneficial for urinalysis with low-cost, enabling the use of micro-volumes of samples, high reproducibility, high selectivity, and good stability.

## Acknowledgment

The authors acknowledge financial support from the Petchra Pra Jom Klao Ph.D. Research Scholarship, Innovation and Partnerships Office, King Mongkut's University of Technology Thonburi.

## Supporting Information

Supporting Information is available at https://doi.org/10.33961/jecst.2019.00206

## References


[1] A. Hogkinson, "Oxalic acid in biology and medicine", New York: Academic press, **1977**, pp. 104-158.
[2] C.S. Pundir, N.K. Kuchhal, and M.S. Thakur, *Indian J. Biochem. Biophys.*, **1998**, *35(2)*, 120-122.
[3] C.S. Pundir, and M.S. Thaku, *Clin. Chem.*, **1998**, *44(6)*, 1364-1365.
[4] D.L. Earnest, G. Johnson, H.E. Williams, and W.H. Admirand, *Gastroenterol*, **1974**, *66(6)*, 1114-1122.
[5] L. Yang, H. Jianshe, W. Dawei, H. Haoqing, and Y. Tianyan, *Anal. Methods*, **2010**, *2(7)*, 855-859.
[6] C. Fua, L.X. Wang, and Y.Z. Fang, *Talanta*, **1999**, *50(5)*, 953-958.
[7] D.R. Skotty, and T.A. Nieman, *J. Chromatogr.*, **1995**, *665(1)*, 27-36.
[8] A.A. Ensafi, and A. Kazemzadeh, *Fresenius J. Anal. Chem.*, **2000**, *367(6)*, 590-592.
[9] A. Mokhtari, M. Keyvanfard, and I. Emami, *RSC Adv*, **2015**, *5(37)*, 29214-29221.
[10] S. Peldszus, P.M. Huck, and S.A. Andrews, *J. Chromatogr. A*, **1998**, *793(1)*, 198-203.
[11] E.F. Perez, G.O. Neto, and L.T. Kubota, *Sens. Actuators, B*, **2001**, *72(1)*, 80-85.
[12] Y.Y. Zhang, X.Y. Bai, X.M. Wang, K.K. Shiu, Y. Zhu, and H. Jiang, *Anal. Chem.*, **2014**, *86(19)*, 9459-9465.
[13] Y.H. Fu, Y.P. Lin, T.S. Chen, and L.S. Wang, *J. Electroanal. Chem.*, **2012**, *687*, 25-29.
[14] T.A. Ivandini, T.N. Rao, A. Fujishima, and Y. Einaga, *Anal. Chem.*, **2006**, *78(10)*, 3467-3471.
[15] Z. Yanqiong, Y. Changzhu, P. Wenhong, and Z. Jingdong, *Food Chem.*, **2009**, *114(4)*, 1523-1528.
[16] C.M. Welch, and R.G. Compton, *Anal. Bioanal. Chem.*, **2006**, *384(3)*, 601-619.
[17] L.G. Shaidarova, and G.K. Budnikov, *J. Anal. Chem.*, **2008**, *63*, 922-942.
[18] M. Oyama, *Anal. Sci.*, **2010**, *26(1)*, 1-12.
[19] M. J. Chollier-Brym, F. Epron, E. Lamy-Pitara, and J. Barbier, *J. Electroanal. Chem.*, **1999**, *474(2)*, 147-154.
[20] S. N. Pron'kin, O. A. Petrii, G. A. Tsirlina, and D. J. Schiffrin, *J. Electroanal. Chem.*, **2000**, *480(1-2)*, 112-119.
[21] L. C. Rockombeny, J. P. Feraud, B. Queffelec, D. Ode, and T. Tzedakis, *Electrochim. Acta*, **2012**, *66*, 230-238.
[22] H. J. Wang, M. Imura, Y. Nemoto, S. E. Park, and Y. Yamauchi, *Chem. Asian J.*, **2012**, *7(4)*, 802-808.
[23] J. Y. Shin, Y. S. Kim, Y. Lee, J. H. Shim, C. Lee, and S. G. Lee, *Chem. Asian J.*, **2011**, *6(8)*, 2016-2021.
[24] S. J. Guo, D. Wen, Y. M. Zhai, S. J. Dong, and E. K. Wang, *ACS Nano*, **2010**, *4(7)*, 3959-3968.
[25] E. Yoo, T. Okata, T. Akita, M. Kohyama, J. Nakamura, and I. Honma, *Nano Lett.*, **2009**, *9(6)*, 2255-2259.
[26] A. Iwan, M. Malinowski, and G. Pasciak, *Renew. Sustain. Energy Rev.*, **2015**, *49*, 954-967.
[27] N. Seselj, C. Engelbrekt, and J. Zhang, *Sci. Bull.*, **2015**, *60(9)*, 864-876.
[28] E. Quesnel, F. Roux, F. Emieux, P. Faucherand, E. Kymakis, G. Volonakis, F.Giustino, B. Martín-Garía, I. Moreels, and S.A. Gürsel, *2D Mater.*, **2015**, *2(30204)*, 1-16.
[29] A. Marinkas, F. Arena, J. Mitzel, G.M. Prinz, A. Heinzel, V. Peinecke, and H. Natter, *Carbon*, **2013**, *58*, 139-150.
[30] S. Park, Y. Shao, H. Wan, P.C. Rieke, V.V. Viswanathan, S.A. Towne, L.V. Saraf, W.J. Liu, Y. Lin, and Y. Wang, *Electrochem. Commun.*, **2011**, *13(3)*, 258-261.
[31] K. Income, N. Ratnarathorn, N. Khamchaiyo, C. Srisuvo, L. Ruckthong, and W. Dungchai, *Int. J. Anal. Chem.*, **2019**, 1-11.
[32] S. Chutipongtanate, and V. Thongboonkerd, *Anal. Biochem.*, **2010**, *402(1)*, 110-112.
[33] A.J. Bard, and L.R. Faulkner, "Fundamentals and Applications: Electrochemical Methods", Wiley, New York, **2001**.
[34] C.O. Laoire, S. Mukerjee, K.M. Abraham, E.J. Palichta, and M.A. Hendrickson, *J. Phys. Chem. C*, **2009**, *113(46)*, 20127-20134.
[35] R.B. Keithley, P. Takmakov, E.S. Bucher, A.M. Belle, C.A. Owesson-White, J. Park, and R.M. Wightman, *Anal. Chem.*, **2011**, *83(9)*, 3563-3571.
[36] X. Cao, X. Cai, Q. Feng, S. Jia, and N. Wang, *Anal. Chim. Acta*, **2012**, *752*, 101-105.
[37] G.W. Latimer, "Guidelines for Standard Method Performance Requirements: Official Methods of Analysis", 20th ed, United States: AOAC International, **2016**, pp. 1-7.
[38] T. A. Ivandini, T. N. Rao, A. Fujishima, and Y. Einaga, *Anal. Chem.*, **2006**, *78(10)*, 3467-3471.
[39] T. C. Canevari, J. Arguello, M. S. P. Francisco, and Y. Gushikem, *J. Electroanal. Chem.*, **2007**, *609(2)*, 61-67.
[40] F. Manea, C. Radovan, I. Corb, A. Pop, G. Burtica, P. Malchev, S. Picken, and J. Schoonman, *Sensors*, **2007**, *7(4)*, 615-627.
[41] H. Ahmar, A. R. Fakhari, M. R. Nabid, S. J. T. Rezaei, and Y. Bide, *Sens. Actuators B Chem.*, **2012**, *171*, 611-618.
[42] A. R. Fakhari, B. Rafiee, H. Ahmar, and A. Bagheri, *Anal. Methods*, **2012**, *4(10)*, 3314-3319.
[43] S. Lei, Z. Faqiong, and Z. Baizhao, *Electroanalysis*, **2013**, *25(2)*, 453-459.
[44] C. Xiaomei, C. Zhixiong, H. Zhiyong, O. Munetaka, J. Yaqi, and C. Xi, *Nanoscale*, **2013**, *5(13)*, 5779-5783.
[45] T. Maiyalagan, P. Kannan, M. J. Niedziolka, and J. N. Jönsson, *Anal. Chem.*, **2014**, *86(15)*, 7849-7857.
[46] J. B. Raoof, F. Chekin, and V. Ehsani, *Sens. Actuators B Chem.*, **2015**, *207*, 291-296.
[47] W. Xiaofeng, C. Yong, Y. Zheng, S. Hailiang, G. Shixing, L. Jun, and S. Wei, *Ionics.*, **2015**, *21(3)*, 877-884.
[48] L. Dandan, W. Yaoxian, and Z. Ganqing, *Int. J. Electrochem. Sci.*, **2015**, *10*, 6794-6802.
[49] M. Le, Z. Qiang, Z. Min, W. Lishi, and C. Faliang, *J. Exp. Nanosci.*, **2016**, *11(16)*, 1242-1252.